ISSN: 0976-3031

Available Online at http://www.recentscientific.com

CODEN: IJRSFP (USA)

International Journal of Recent Scientific Research
Vol. 9, Issue, 5(J), pp. 27199-27206, May, 2018

International Journal of Recent Scientific Research

DOI: 10.24327/IJRSR

Research Article

IMMOBILIZATION AND CHARACTERIZATION OF L-ASPARAGINASE EXTRACTED FROM *SOLANUM NIGRUM* ON MAGNETIC NANOPARTICLES

Jagjit Kaur[1]., Raman Kumar[2] and Kuldeep Kumar[3]*

[1,2]Department of Biotechnology, Maharishi Markandeshwar (Deemed to be University), Mullana, Haryana, India
[3]Department of Biotechnology, Multani Mal Modi College, Patiala, Punjab, India

DOI: http://dx.doi.org/10.24327/ijrsr.2018.0905.2209

ARTICLE INFO

Article History:
Received 12th February, 2018
Received in revised form 9th March, 2018
Accepted 26th April, 2018
Published online 28th May, 2018

Key Words:

L-asparaginase, magnetic nanoparticles, immobilization, characterization.

ABSTRACT

L-asparaginase is an anti-tumor enzyme used for the treatment of Acute Lymphoblastic Leukemia (ALL), a disease caused by expansion of lymphoid blasts in bone marrow and blood. L-asparaginase is produced by a variety of sources like bacteria, fungus, yeast and plants. *S. nigrum* is one potent source of L-asparaginase with enzyme activity of 52 IU/ml. To increase the stability and shelf-life of L-asparaginase, it was immobilized on different nanoparticles like magnetic, ZnO, starch and alginate. The synthesized nanoparticles were characterized using UV-visible spectroscopy, Fluorescence spectroscopy and Scanning Electron Microscopy (SEM). It was found that λ_{max} of magnetic nanoparticles was 380 nm, ZnO nanoparticles was 360 nm and for starch and alginate nanoparticles it was 280 nm and 400 nm respectively. FTIR spectra showed different vibrational and stretching bonds involved during formation of nanoparticles. The size of magnetic nanoparticles was 25 nm and for ZnO nanoparticles was 300 nm after immobilization of L-asparaginase. The immobilization of L-asparaginase on starch and alginate nanoparticles was not found to be efficient. Magnetic nanoparticles were further characterized kinetically. The K_m and V_{max} for L-asparaginase loaded magnetic nanoparticles was 7.11 mM and 100 µM/min respectively. The optimum pH was 8.0 and temperature was 50 ℃. The metal ions have both inhibitory and enhancing effect on L-asparaginase activity chelators mostly enhanced the activity. Therefore, L-asparaginase immobilized on magnetic nanoparticles could be further used in applications like drug delivery.

INTRODUCTION

L-asparaginase is a well-known enzyme used for the treatment of Acute Lymphoblastic Leukemia (ALL), a type of cancer in children arising due to expansion of lymphoid blasts and monoclonal proliferation in blood and bone marrow[1-2]. Normal cells can synthesize asparagine on their own, but the cancer cells depend on extracellular supply of asparagine from the blood. When L-asparaginase is injected into the blood it breaks down asparagine to aspartic acid and ammonia depriving the cancer cells of asparagine. Hence, the cancer cells die due to asparagine starvation[3]. L-asparaginase is produced by a number of bacteria[4-10], fungus[11], yeast[12], actinomycetes and plants[13-21]. One of the recently discovered potent sources of L-asparaginase is *Solanum nigrum*[21-22]. It is known by different names such as European black nightshade, garden huckleberry, petty morel, hound's berry, popolo, duscle, wonder berry and garden nightshade[23-24]. It is short-lived perennial shrub mainly found in Eurasia, South Africa, Australia and America. Cooked leaves and ripe berries are used as food and its different parts are used as medicine[25]. The plant may grow upto the height of 30-120 cm. Its leaves are 2-5 cm wide and 4-8 cm long which may be hairy or hairless, heart-shaped, ovate, have large-toothed or wavy edges. The fruits are 6-8 mm diameter and appear to be dull black to purple black[26] or red on ripening[27] (Figure 1).

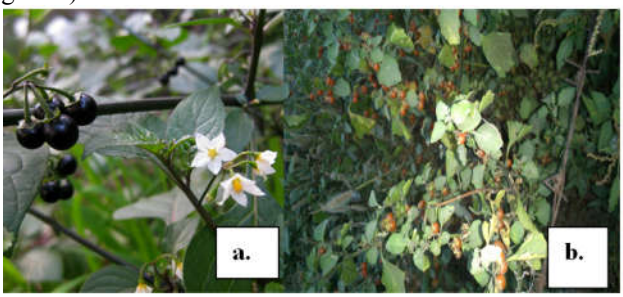

Figure 1 *Solanum nigrum* (a. black fruits, b. red fruits)

L-asparaginase extracted from plant *S. nigrum* is stable over wide range of environmental conditions and have higher

Corresponding author:* **Kuldeep Kumar
Department of Biotechnology, Multani Mal Modi College, Patiala, Punjab, India

enzyme activity as compared to its microbial counterparts[22]. Therefore, it could find its application in medical and food industry. However, free enzymes can easily be degraded, inhibited or irreversibly denatured[28-29]. On immobilization enzyme-substrate interaction changes the kinetic parameters of enzyme and hence increases enzyme activity, stability and shelf-life[30-31]. Nanoparticles have been a major interest area for last few years and have been used to immobilize enzymes as they offer a number of advantages such as increased shelf life, activity, stability, large surface area, electronic properties and reusability[32]. Enzyme loaded nanoparticles have been used for fabrication of biosensors and as antibacterial agents[33].

In our present study we extracted L-asparaginase from *S. nigrum* and immobilized it onto different nanoparticles like magnetic, zinc oxide, starch and alginate nanoparticles. The synthesized L-asparaginase loaded nanoparticles were characterized using SEM, FTIR, UV-visible spectroscopy and effect of pH, temperature, metal ions, chelators and substrate concentration was studied on them.

MATERIALS AND METHODS

Extraction of Enzyme

L-asparaginase was extracted from different parts of *S. nigrum* according to the method previously described[13]. Briefly, the different parts from the plants were collected and then washed with distilled water. The parts were homogenized with 0.15 M KCl buffer and centrifuged at 8,000 rpm for 20 min at 4 °C. The supernatant thus obtained was taken as the crude extract. The presence of L-asparaginase in crude extract was monitored using nesselerization method.

Immobilization of Isolated L-asparaginase Using Different Nanoparticles

The crude extract obtained from the selected plant was immobilized using the following method:

Magnetic nanoparticles

The magnetic nanoparticles were prepared by the following method: 2.43 g $FeCl_2.4H_2O$, 0.99 g $FeCl_3.6H_2O$, 6 ml ammonia hydroxide (25 %) was added to 80 ml deionized water. The solution was sonicated for 1 hr at 20 kHz using ultrasonicator (Sonics Vibra Cell). The precipitates were centrifuged at 8,000 rpm for 15 min (Sigma 2-16 PK) washed thrice and then redispersed in 100 ml deionized water. 10 ml chitosan (1%) and 800 µl of enzyme was added to the above solution and stirred for 24 hrs. The black colored precipitates were collected using permanent magnets and dried in oven[33].

Zinc oxide nanoparticles

KOH solution (0.4 M) was added slowly to $Zn(NO_3)_2.6H_2O$ (0.2 M) solution (both prepared in deionized water) under vigorous stirring at room temperature. A white colored suspension was formed which was centrifuged at 5,000 rpm for 20 min. The precipitates were washed thrice with deionized water and then with absolute ethanol. The precipitates were then calcined at 500 °C for 3 hrs[34].

Starch nanoparticles

15 g starch was dissolved in 100 ml $ZnCl_2$ solution (65%) with continuous stirring (500 rpm) and heating (80 °C). To the above solution NaOH (15 %) was added drop-wise with continuous stirring at 500 rpm till the final pH of mixture was 8.4. The mixture was aged by stirring it for 30 min at 500 rpm and 80 °C. The nanocomposites formed were calcined at 575 °C for 1 hr to obtain nanoparticles[35].

Alginate nanoparticles

10 ml sodium alginate (1 %) solution was prepared in deionized water and added to 20 ml zinc acetate (3 %) through syringe with 0.49 mm diameter stainless steel needle under continuous stirring on magnetic stirrer. The beads formed are hardened for 30 min with gentle stirring. Beads were then separated and dried in crucible[36].

Characterization of L-asparaginase Loaded Nanoparticles

The λ_{max} for nanoparticles was calculated using UV-visible spectrophotometer (PC Based Double Beam Spectrophotometer 2202, Systonics). Functional groups were studied using Fourier Transform Infrared Spectroscopy (Carry 630 FTIR spectrophotometer, Agilent Technologies, USA) and surface morphology was determined using Scanning Electron Microscope (SEM) (JEOL, JSM-6010LV, USA).

Kinetic Characterization of L-asparaginase Loaded Nanoparticles

The effect of substrate (asparagine) concentration (10^{-1} to 10^{-10} M), pH (5.5, 6.0, 6.5, 7.0, 7.5, 8.0, 8.5, 9.0 and 9.5), temperature (25, 30, 35, 40, 45, 50, 55, 60, 65, 70 and 75 °C), metal ions (10 mM of each Ca^{2+}, K^{+}, Cu^{2+}, Na^{+}, Mn^{2+}, Mg^{2+}, Co^{2+} and Hg^{2+}) and chelators [5 mM of each ethylenediaminetetraacetic acid (EDTA), urea, sodium dodecyl sulfate (SDS), β-mercaptoethanol (β-ME) and Triton-X 100] on the activity of immobilized enzyme was studied.

RESULTS AND DISCUSSIONS

L-asparaginase Activity of Different Parts of S. nigrum

It was seen that leaves contain more amount of enzyme as compared to stem, roots and flowers/fruits. Enzyme activity of leaves of *S. nigrum* was found to be 52.00 ± 0.01 IU/ml. The least activity was shown by roots 20.52 ± 0.34 IU/ml whereas that of stem and fruits/flowers was 35.46 ± 1.39 IU/ml and 39.35 ± 0.46 IU/ml respectively. Since the L-asparaginase extracted from leaves showed highest enzyme activity, therefore, it was used for further experiments.

Immobilization of Isolated L-asparaginase Using Different Nanoparticles

L-asparaginase extracted from leaves of *S. nigrum* was immobilized on magnetic, ZnO, starch and alginate nanoparticles.

Characterization of L-asparaginase loaded nanoparticles

λ_{max} of nanoparticles

The λ_{max} of different nanoparticles loaded with L-asparaginase is given in figure 2. Characterization of magnetic nanoparticles was done by using UV-visible spectroscopy and it was found that λ_{max} of magnetic nanoparticles was 380 nm. The results were similar to magnetic nanoparticles synthesized by wet synthesis method showed the maximum absorbance at 370 nm[37]. Similarly, the magnetic nanoparticles synthesized by

precipitation method had λ_{max} at 272 nm[38]. ZnO nanoparticles synthesized by reducing $Zn(NO_3)_2.6H_2O$ with KOH solution under vigorous stirring and collecting the precipitates by thermal decomposition showed maximum absorbance at 360 nm. The λ_{max} of ZnO nanoparticles synthesized by Guo and Yang[39] was found to be at 300 nm. ZnO nanoparticles synthesized by thermal decomposition had λ_{max} at 400 nm[40] and 364 nm[41]. The λ_{max} for starch nanoparticles was at 280 nm. In a study, drug-loaded starch nanoparticles were characterized, and their maximum absorption was found at 277 nm[42]. In another study the λ_{max} of starch nanoparticles was observed to be at 540 nm[43]. Alginate nanoparticles were synthesized by adding sodium-alginate in zinc acetate solution through a stainless-steel needle. The beads were collected and dried in crucible. The nanoparticles were characterized by measuring their absorbance between 200-500 nm. Their λ_{max} was found at 400 nm which indicated the formation of alginate nanoparticles. Alginate nanoparticles were synthesized and loaded with paclitaxel for breast cancer. The λ_{max} for alginate nanoparticles was 280 nm[44].

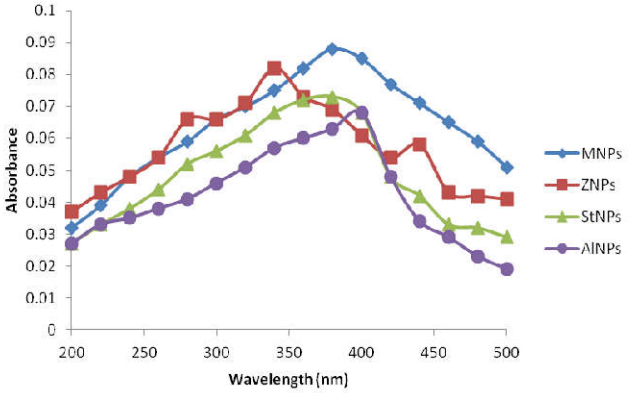

Figure 2 λ_{max} of L-asparaginase loaded nanoparticles

FTIR spectra of nanoparticles

The chemical bonds and functional groups can be identified using FTIR because every bond has a specific energy absorption band[45]. The nanoparticles were taken in powdered form and FTIR spectra were collected from 400-4000 cm^{-1}. The FTIR spectra of magnetic nanoparticles showed peaks at 3729, 3054, 2425, 1524 and 573 cm^{-1} with a prominent peak at 573 cm^{-1} due to stretching vibration of Fe-O which indicates the formation of magnetic nanoparticles. The peaks from 1500-3700 cm^{-1} due to stretching of C=O bond. Tharani and Nehru[38] characterized magnetic nanoparticles and they found peak due to -OH stretching at 552 cm^{-1} and from 1700-3600 cm^{-1} due to C=O stretching. In a study on chitosan-coated magnetic nanoparticles a characteristic peak was observed at 570 cm^{-1} which was due to magnetic nanoparticles[46]. The enzyme extracted from *S. nigrum* was immobilized on magnetic nanoparticles and it was found that the peak shifted from 573 to 567 cm^{-1} which indicates the immobilization of enzyme on magnetic nanoparticles. The peaks from 1500-3700 cm^{-1} were due to C=O stretching vibration (Figure 3a).

The FTIR spectra of ZnO nanoparticles showed peaks at 502, 612 and 685 cm^{-1} which are due to Zn-O bond[41, 47-48]. The stretching of Zn-O bond gives the peak at 502 cm^{-1} which indicated the formation of ZnO nanoparticles[41]. The bonds at 1405 and 1537 cm^{-1} are due to presence of water[48]. The FTIR spectrum of L-asparaginase immobilized on ZnO nanoparticles was found to be similar to bare ZnO nanoparticles which indicate that plant enzyme does not interfere much with morphology of nanoparticles and gets immobilized with ease (Figure 3b). The peaks at 474 and 673 cm^{-1} are due to Zn-O stretching bond, whereas, peaks at 1415 and 1540 cm^{-1} are due to water and carboxyl groups. Similar results were found by Verma *et al.*[49].

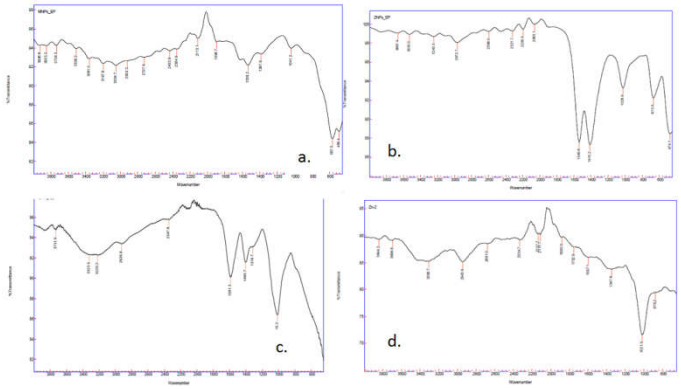

Figure 3 FTIR spectrum of L-asparaginase loaded nanoparticles (a) magnetic, (b) ZnO, (c) starch and (d) alginate nanoparticles

The FTIR spectra of starch nanoparticles depict peaks at 1011, 1574, 2870 and 3347 cm^{-1}. C-O stretching formed peak at 1011 cm^{-1} and that at 1574 cm^{-1} was due to bound water in starch. C-H stretching gave peak at 2870 cm^{-1} whereas O-H vibrational stretching gave peak at 3347 cm^{-1}. Similar results were observed by Simi and Abraham[50]. They obtained the pinnacles at 1016 cm^{-1} (O-C stretching), 1645 cm^{-1} (bound water), 2926 cm^{-1} (C-H stretching) and 3390 cm^{-1} (O-H vibrational stretching). The presence of C-O bonds can be observed at 1000-1200 cm^{-1} [51-52]. On immobilization of L-asparaginase extracted from *S. nigrum* the peak at 1574 cm^{-1} moved to 1591 cm^{-1} whereas that at 2870 cm^{-1} moved to 2926 cm^{-1} (Figure 3c). The peak for bound water was found at 1015 cm^{-1} and for O-H stretching was at 3323 cm^{-1}. The results were similar to those found in earlier studies[50].

For alginate nanoparticles clear and sharp epitomes at 1037 cm^{-1}, 2956 cm^{-1} and 3691 cm^{-1} could be visualized. The pinnacle at 1037 cm^{-1} could be because of C-O-C stretching and that at 2956 cm^{-1} to C-H bonds. The O-H stretching gave peaks from 3200-3800 cm^{-1}. The results were similar to that obtained by Kyziol *et al.*[53] who synthesized alginate/chitosan formulation for controlled delivery of ciprofloxacin. A peak at 1021 cm^{-1} was obtained due to C-O-C stretching and 2845 cm^{-1} due to C-H stretching[53]. L-asparaginase isolated from *S. nigrum* and immobilized on alginate nanoparticles had spectrum with peaks at 1021 cm^{-1}, 2943 cm^{-1} and few peaks from 3300-3800 cm^{-1} (Figure 3d). The peak due to C-O-C stretching shifted from 1037 to 1021 cm^{-1} which was similar to study conducted by Kyziol *et al.*[53] This indicated the coating of L-asparaginase on alginate nanoparticles. The further peaks from 1200-3800 cm^{-1} are not quite distinct which may be due to improper enzyme immobilization.

SEM images of nanoparticles

The synthesized nanoparticles were characterized using SEM and it was found that magnetic nanoparticles were spherical in shape and were nearly 13 nm. Similar results were found by Bonini *et al.*[55] where the size of synthesized nanoparticles was

15-20 nm. In a study conducted by Chin and Yaacob[56] it was found that three different sized nanoparticles were synthesized with size 3.5 nm, 5.1 nm and 9.7 nm. Magnetic nanoparticles were synthesized using two-step desolvation method and it was found that four different sized nanoparticles (122, 136, 234 and 237 nm) were synthesized[57]. Magnetic nanoparticles of 266.1 nm were synthesized by Wang *et al*.[58] The synthesized magnetic nanoparticles were coated with L-asparaginase extracted from *S. nigrum* and SEM images indicated successful coating of enzyme as the size of nanoparticles increased to 25 nm (Figure 4a). Moreover, the enzyme coated nanoparticles formed agglomerates of nearly 150-250 nm. Similar results were found in a study where magnetic nanoparticles of 5-15 nm were synthesized with 10 nm coating of polydopamine. The polydopamine coated magnetic nanoparticles formed aggregates of 50-250 nm[59]. Spherically shaped magnetic nanoparticles coated with peroxidase extracted from *Euphorbia tirucalli* were synthesized[60].

SEM images of ZnO nanoparticles indicate formation of 50-60 nm sized nanoparticles. The nanoparticles range from spherical shape to flakes. ZnO nanoparticles of spherical shape and sizes 4.0, 3.6, 2.8 and 2.6 nm were synthesized by Guo and Yang[39]. Nearly spherical shaped ZnO nanoparticles with diameter more than 400 nm were synthesized[61]. The formation of nanoflakes was observed in SEM images when thermal decomposition was used to synthesize ZnO nanoparticles[40]. 27-82 nm sized and well isolated nanoparticles were synthesized by Arora *et al*.[48] ZnO nanoparticles of 50 nm were synthesized by Krithika *et al*.[41] SEM images indicated that coating of ZnO nanoparticles with L-asparaginase extracted from *S. nigrum* increased their size to 300 nm (Figure 4b). The enzyme coated irregularly on ZnO nanoparticles increasing their size tremendously. The aggregation of nanoparticles may be due to high surface energy[62]. In another study 150-200 nm sized nanoparticles were synthesized using potato extract[49].

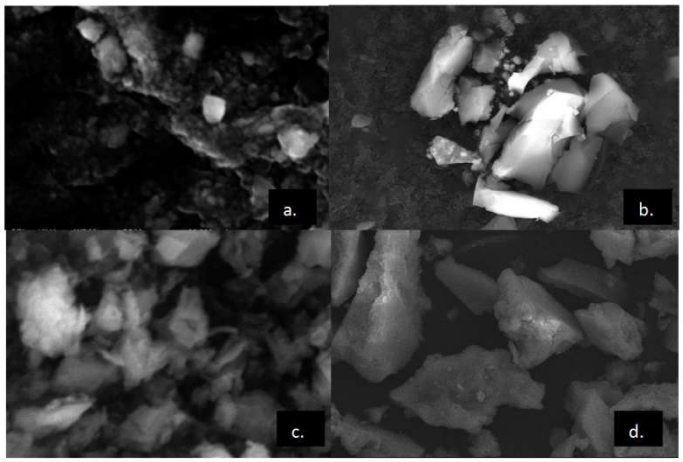

Figure 4 SEM images of L-asparaginase loaded nanoparticles (a) magnetic, (b) ZnO, (c) starch and (d) alginate nanoparticles

The size of starch nanoparticles was 300 nm and the nanoparticles were irregular in shape. This may be attributed to large size of polymer. Different nanoparticles were synthesized using waxy corn starch with the average particle size of 20-60 nm[51]. Starch nanoparticles were synthesized and modified with deoxycholic acid. They were characterized using SEM and their average size was 182-247 nm[63]. Acetylated starch nanoparticles with average diameter of 500 nm were synthesized by Teodoro *et al*.[64] In another study starch nanoparticles were synthesized and modified with 2,2,6,6-tetramethylpiperidine-1-oxyl (TEMPO) having 50 nm diameter[65]. When L-asparaginase extracted from *S. nigrum* was immobilized on starch nanoparticles size increased from 300 nm to 350 nm (Figure 4c). The coating of enzyme on nanoparticles was uneven and irregular making their imaging very difficult.

The size of alginate nanoparticles was found to be 400 nm which increased to 450 nm upon immobilization of L-asparaginase on them (Figure 4d). Calcium-alginate nanoparticles were synthesized using cross-linking method and average diameter of synthesized nanoparticles was 350 nm[54]. In another study alginate nanoparticles were synthesized for loading paclitaxel and their size was found to be 200 nm[66]. After immobilization the size of nanoparticles increased which indicated that immobilization was successful.

The λ_{max}, FTIR spectra and SEM images indicate that magnetic nanoparticles were suitable for further study therefore, they were kinetically characterized.

Kinetic Characterization of L-asparaginase Immobilized on Magnetic Nanoparticles

Effect of substrate concentration

The K_m of L-asparaginase immobilized on magnetic nanoparticles was 7.11 mM and V_{max} was 100 µM/min (Figure 5). In comparison to free enzyme the V_{max} of immobilized enzyme has increased which makes it suitable matrix for immobilization. This could be due to the fact that enzyme has been confined to a limited space which increases the interaction between enzyme and substrate[67-68]. Peroxidase enzyme from *E. tirucalli* was immobilized on magnetic nanoparticles with K_m 9.53 mM[60].

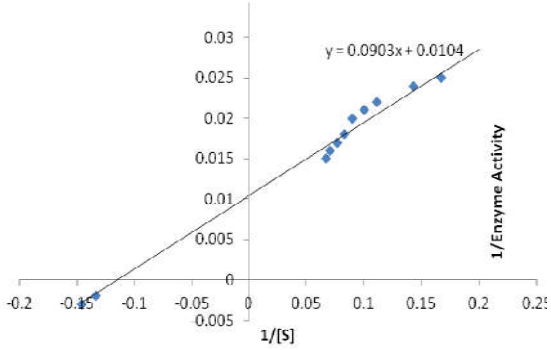

Figure 5 Double reciprocal graph for L-asparaginase extracted from *S. nigrum* immobilized on magnetic nanoparticles

Effect of pH

L-asparaginase extracted from *S. nigrum* and immobilized on magnetic nanoparticles was characterized over a range of pH (5.5 to 9.5) and optimum pH was found to be 8.0 (Figure 6). After immobilization the enzyme can remain active over alkaline pH which is expected to be necessary for L-asparaginase activity. The changes in pH could be due to interaction of charged group's enzyme with stationary charges of magnetic nanoparticles. Peroxidase enzyme from *E. tirucalli* was immobilized on magnetic nanoparticles and its optimum pH for free enzyme was 5.5 and for immobilized one was 6.0[60].

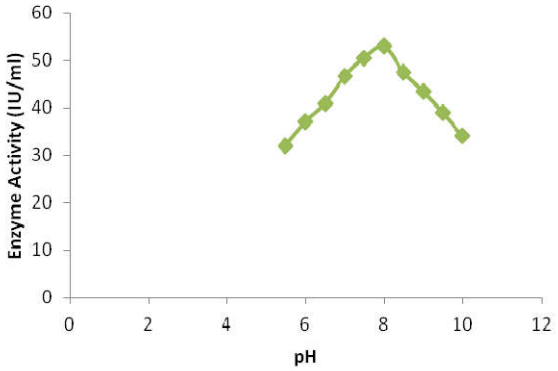

Figure 6 Effect of pH for L-asparaginase extracted from *S. nigrum* immobilized on magnetic nanoparticles

Effect of temperature

L-asparaginase isolated from *S. nigrum* was studied thermally by checking its activity at different temperatures (25-75 °C) and it showed highest activity at 50 °C (Figure 7). The optimum temperature for immobilized enzyme was thermally stable than free enzyme (35 °C) because denaturation and aggregation of free enzyme occurs easily as compared to immobilized enzyme[69]. The optimum temperature for immobilized peroxidase enzyme from *E. tirucalli* on magnetic nanoparticles was 55 °C[60].

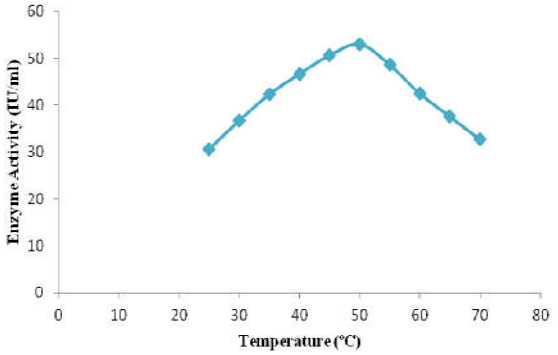

Figure 7 Effect of temperature for L-asparaginase extracted from *S. nigrum* immobilized on magnetic nanoparticles

Effect of metal ions

The effect of different metal ions (10 mM) was studied on L-asparaginase from *S. nigrum* and immobilized on magnetic nanoparticles. It was found that Hg^{2+}, Mg^{2+}, Mn^{2+} and Cu^{2+} showed inhibitory effect on L-asparaginase activity (Figure 8). Ca^{2+}, K^{+}, Na^{+} and Co^{2+} ions enhanced the activity with K^{+} ions having the highest positive effect by 55 %. The loss in enzyme activity is due to conformational changes in enzyme caused by metal ions[70]. Moreover, immobilized enzyme is more stable to metal ions than free enzyme, which may be attributed to confinement of enzyme to specific membrane space[71-72].

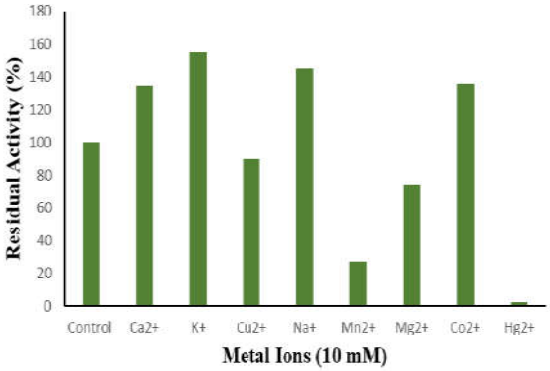

Figure 8 Effect of metal ions for L-asparaginase extracted from *S. nigrum* immobilized on magnetic nanoparticles

Effect of chelators

Effect of different chelators was studied on L-asparaginase activity and it was found that urea, SDS and Triton-X 100 inhibited L-asparaginase activity with urea as the strongest inhibitor (Figure 9). On the other hand, EDTA and β-ME enhanced activity with retaining 30 and 15 % residual activity respectively. This is due to binding of chelators to enzyme and causing conformational changes in it. Immobilization provided more tolerance to enzyme as inhibitory effect is more in free enzyme as compared to immobilized enzyme.

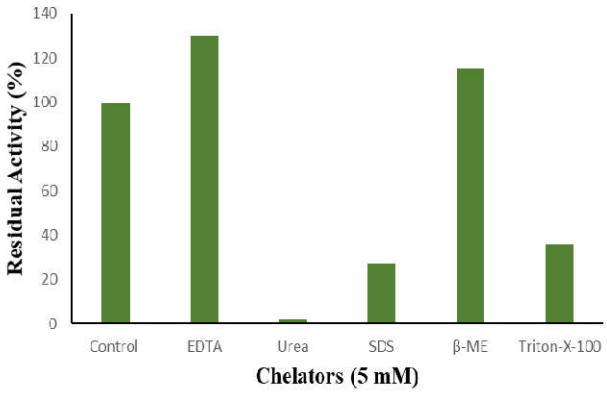

Figure 9 Effect of chelators for L-asparaginase extracted from *S. nigrum* immobilized on magnetic nanoparticles

CONCLUSIONS

L-asparaginase is produced by a number of sources out of which *S. nigrum* show a significant amount of L-asparaginase activity. The amount of L-asparaginase is different for different parts of the plant with leaves possessing the highest activity 52 IU/ml. free enzyme is susceptible to degradation and loss of enzyme activity. This could be overcome by immobilizing the enzyme into suitable matrix. Nanoparticles serve as a material of choice for immobilizing enzymes. In the present study L-asparaginase was immobilized onto magnetic, ZnO, starch and alginate nanoparticles. It is evident that due to larger size of starch and alginate they do not prove to be suitable matrix for immobilization. On the other hand, magnetic nanoparticles synthesized were 25 nm and could be used for immobilizing L-asparaginase efficiently. The enzyme was kinetically characterized, and it was found that it was much stable to experimental conditions exposed when compared to previous studies.

References

1. Fullmer A, O'Brien S, Kantarjian H, Jabbour E. Emerging therapy for the treatment of acute lymphoblastic leukemia. *Expert Opin. Emerg. Drugs*. 2010; 15 (1): 1-11.
2. Shrivastava A, Khan AA, Khurshid M *et al*. Recent developments in L-asparaginase discovery and its potential as anticancer agent. *Crit. Rev. Oncol./Hematol.* 2016; 100: 1-10.
3. Kumar K, Kaur J, Walia S, Pathak T, Aggarwal D. L-asparaginase: an effective agent in the treatment of acute lymphoblastic leukemia. *Leuk*. *Lymphoma*. 2013; 55 (2): 256-262.
4. Netrval J. Stimulation of L-asparaginase production in *E. coli* by organic and amino acids. *Folia Microbiol*. 1977; 22: 106-116.
5. Maladkar NK, Singh VK, Naik SR. Fermentative production and isolation of L-asparaginase from *Erwinia caratovora,* EC 113. *Hindustan Antibiot. Bull.* 1993*;* 35: 77-86.
6. Stark RM, Suleiman MS, Hassan IJ, Greenman J, Millar MR. Amino acid utilization and deamination of glutamine and asparagine by *Helicobacter pylori.* J. Med. Microbiol. 1997; 46: 793-800.
7. Prista AA, Kyriakidis DA. L-asparaginase of *Thermus thermophilus*: purification, properties and identification of essential amino acids for its catalytic activity. *Molecul. Cellul. Biochem*. 2001; 216 (1-2): 93-101.
8. Kavitha A, Vijayalakshmi M. Optimization and purification of L-asparaginase produced by *Streptomyces tendae* TK-VL_333. Zeitschrift fur Naturforschung C. 2010; 65 (7-8): 528-531.
9. Ghosh S, Murthy S, Govindasamy S, Chandrasekaran M. Optimization of L-asparaginase production by *Serratia marcescens* (NCIM 2919) under solid state fermentation using coconut oil cake. *Sustain. Chem. Process*. 2013; 1: 1-8.
10. Shirazian P, Asad S, Amoozegar MA. The potential of halophilic and halotolerant bacteria for the production of antineoplastic enzymes: L-asparaginase and L-glutaminase. *Exp. Clin. Sci. Int. Online J. Adv. Sci.* 2016; 15: 268-279.
11. Mishra A. Production of L-asparaginase, an anticancer agent, from *Aspergillus niger* using agricultural waste in solid state fermentation. *Appl. Biochem. Biotechnol.* 2006; 135 (1): 33-42.
12. Bon EPS, Carvajal E, Stambrough M, Magasanik B. Asparaginase II of *Saccharomyces cerevisiae*. GLN3/URE2 regulation of a periplasmic enzyme. *App. Biochem. Biotechnol*. 1997; 63-65: 203-212.
13. Bano M, Sivaramakrishnan VM. Preparation and properties of L-asparaginase from green chillies (*Capsicum annum* L.). J. Biosci. 1980; 2 (4): 291-297.
14. Siechiechowicz K, Ireland R. Isolation and properties of an asparaginase from leaves of *Pisum sativum*. *Phytochem*. 1989; 28: 2275.
15. Borek D, Podkowinski J, Kisiel A, Jaskolski M. Isolation and characterization of cDNA encoding L-asparaginase from *Lupinus luteus*. *Plant Physiol*. 1999; 119: 1568-1570.
16. Oza P, Trivedi D, Parmar P, Subramanian B. *Withania somnifera* (ashwagandha): Novel source of L-asparaginase. *J. Integrat. Plant Biol*. 2009; 51 (2): 201-206.
17. Pardeep SM, Mahmood R, Jagadeesh KS. Screening and characterization of L-asparaginase producing microorganisms from tulsi (*Ocimum sanctum* L.). *Karnataka J. Agri. Sci*. 2010; 23 (4): 660-661.
18. Kumar K, Punia S, Kaur J, Pathak T. Development of plant asparagine biosensor for detection of leukemia. *J. Pharm. Biomed. Sci.* 2013; 35 (35): 1796-1801.
19. Pathak T, Kumar R, Kaur J, Kumar K. Isolation of L-asparaginase from *Cannabis sativa* and development of biosensor for detection of asparagine in leukemic serum samples. *Res. J. Pharm. Technol*. 2014; 7 (8): 850-855.
20. Punia S, Kaur K, Kumar R, Kumar K. Potentiometric biosensor for asparagine detection. *Int. J. Res. Ayurveda Pharm.* 2015; 6 (2): 282-284.
21. Kataria M, Kaur N, Narula R *et al*. L-asparaginase from novel source- *Solanum nigrum* and development of asparagine biosensor. *Pharma Innovat. J.* 2015; 4 (5): 81-84.
22. Kaur J, Kumar R, Kumar K. Comparative characterization of L-asparaginase extracted from plant and microbial sources. *Int. J. Res. Ayurveda Pharma*. 2017; 8 (5): 86-89.
23. Jain R, Sharma A, Gupta S, Sarethy IP, Gabrani R. *Solanum nigrum*: Current perspectives on therapeutic properties. *Alternat. Med. Rev*. 2011; 16 (1): 78-85.
24. Ali NS, Singh K, Khan MI, Rani S. Protective effect of ethanolic extracts of *Solanum nigrum* on the blood sugar of albino rats. *Int. J. Pharm. Sci. Res.* 2010; 1 (9): 97-99.
25. Li J, Li Q, Feng T. Antitumour activity of crude polysaccharides isolated from *Solanum nigrum* on U-14 cervical carcinoma bearing mice. *Phytother. Res.* 2007; 21 (9): 832-840.
26. Muto M, Mulabagal V, Huang HC *et al*. Japan toxicity of black nightshade (*Solanum nigrum*) extracts on *Alternaria brassicicola*, causal agent of black leaf spot of Chinese cabbage (*Brassica pekinensis*). Department of International Agricultural Development, Tokyo University of Agriculture, Sakuragaoka, Setagaya-ku, Tokyo. *J. Phytopathol*. 2006; 154 (1): 45-50.
27. Venkateswarlu J, Rao MK. Inheritance of fruit colour in the *Solanum nigrum* complex. P. *Indian Acad. Sci.- Sec*. B. 1971; 74 (3): 137-141.
28. Sarkar JM, Leonowicz A, Bollag JM. Immobilization of enzymes on clays and soils. *Soils Biol. Biochem*. 1989; 21: 223-230.
29. Marx MC, Kandeler E, Wood M, Wermbter N, Jarvis SC. Exploring the enzymatic landscape: distribution and kinetics of hydrolytic enzymes in soil particlesize fractions. *Soils Biol. Biochem*. 2005; 37: 35-48.
30. Quiquampoix HA. Stepwise approach to the understanding of extracellular enzyme activity in soil. II. Competitive effects on the adsorption of a beta-D-glucosidase in mixed mineral or organo-mineral systems. *Biochimie*. 1987; 69 (6-7): 765-771.
31. Safari SAA, Emtiazi G, Shariatmadari H. Sorption and immobilization of cellulase on silicate clay minerals. *J. Coll. Interf. Sci*. 2005; 290: 39-44.

32. Lee PC, Meisel DJ. Adsorption and surface-enhanced Raman of dyes on silver and gold sols. *J. Phys. Chem. A*. 1982; 86: 3391-3395.
33. Dorniani D, Hussein MZB, Kura AU *et al*. Preparation of Fe_3O_4 magnetic nanoparticles coated with gallic acid for drug delivery. *Int. J. Nanomed*. 2012; 7: 5745-5756.
34. Ghorbani HR, Mehr FP, Pazoki H, Rahmani BM. Synthesis of ZnO nanoparticles by precipitation method. *Orient. J. Chem*. 2015; 31 (2): 1219-1221.
35. Ma J, Zhu W, Tian Y, Wang Z. Preparation of zinc oxide-starch nanocomposite and its application on coating. *Nanoscale Res. Letter*. 2016; 11 (1): 1-9.
36. Baskoutas S, Giabouranis P, Yannopoulos SN *et al*. Preparation of ZnO nanoparticles by thermal decomposition of zinc alginate. *Thin Solid Films*. 2007; 515 (2007): 8461-8464.
37. Chaki SH, Malek TJ, Chaudhary MD, Tailor JP, Deshpande MP. Magnetite Fe_3O_4 nanoparticles synthesis by wet chemical reduction and their characterization. *Adv. Nat. Sci.: Nanosci. Nanotechnol*. 2015; 6: 035009.
38. Tharani K, Nehru LC. Synthesis and characterization of iron oxide nanoparticle by precipitation method. *Int. J. Adv. Res. Phys. Sci.* 2015; 2: 47-50.
39. Guo L, Yang S. Synthesis and characterization of poly(vinylpyrrolidone)-modified zinc oxide nanoparticles. *Chem. Mat.* 2000; 12: 2268-2274.
40. Kumar SS, Venkateswarlu P, Rao VR, Rao GN. Synthesis, characterization and optical properties of zinc oxide nanoparticles. *Int. Nano Letters*. 2013; 3: 1-6.
41. Krithika G, Saraswathy R, Muralidhar M *et al*. Zinc oxide nanoparticles—synthesis, characterization and antibacterial activity. *J. Nanosci. Nanotechnol*. 2017; 17: 5209-5216.
42. El-Naggar ME, El-Rafie, MH, El-Sheikh MA, El-Feky GS, Hebeish A. Synthesis, characterization, release kinetics and toxicity profile of drug-loaded starch nanoparticles. *Int. J. Biol. Macromol*. 2015; 81: 718-729.
43. Ding Y, Zheng J, Zhang F, Kan J. Synthesis and characterization of retrograded starch nanoparticles through homogenization and miniemulsion cross-linking. *Carbohyd. Polym*. 2016; 151: 656-665.
44. Markeb AA, El-Maali NA, Sayed DM *et al*. Synthesis, structural characterization, and preclinical efficacy of a novel paclitaxel-loaded alginate nanoparticle for breast cancer treatment. *Int. J. Breast Cancer*. 2016; 2016: 1-8.
45. Silva JA, Macedo GP, Rodrigues DS, Giordano RLC, Gonc¸alves LRB. Immobilization of *Candida antarctica* lipase B by covalent attachment on chitosan-based hydrogels using different support activation strategies. *Biochem. Eng. J*. 2012; 60: 16-24.
46. Osuna Y, Sandoval J, Saade H *et al*. Immobilization of *Aspergillus niger* lipase on chitosan-coated magnetic nanoparticles using two covalent-binding methods. *Bioproc. Biosys. Eng*. 2015; 38 (8): 1437-1445.
47. Srivastava V, Gusain D, Sharma YC. Synthesis, characterization and application of zinc oxide nanoparticles (n-ZnO). *J. Nanosci. Nanotechnol*. 2013; 39: 9803-9808.
48. Arora AV, Devi S, Jaswal VS *et al*. Synthesis and characterization of ZnO nanoparticles. *Orient. J. Chem*. 2014; 30 (4): 1671-1679.
49. Verma N, Kumar N, Upadhyay LSB, Sahu R, Dutt A. Fabrication and characterization of cysteine-functionalized zinc oxide nanoparticles for enzyme immobilization. *Anal. Letters*. 2017; 50 (11): 1839-1850.
50. Simi CK, Abraham TE. Hydrophobic grafted and cross-linked starch nanoparticles for drug delivery. *Bioproc. Biosys. Eng.* 2007; 30: 173-180.
51. Sun Q, Fan H, Xiong L. Preparation and characterization of starch nanoparticles through ultrasonic-assisted oxidation methods. *Carbohyd. Polym*. 2014; 106: 359-364.
52. Zhigang L, Linrong S, Meina Z. Preparation of starch nanoparticles in a new ionic liquid-in-oil microemulsion. *J. Formul. Sci. Bioavail*. 2017; 1 (1): 1-8.
53. Kyziol A, Mazgala A, Michna J, Regiel-Futyra A, Sebastian V. Preparation and characterization of alginate/chitosan formulations for ciprofloxacin-controlled delivery. *J. Biomat. App*. 2017; 32 (2): 162-174.
54. Nesamony J, Singh PR, Nada SE, Shah ZA, Kolling WM. Calcium alginate nanoparticles synthesized through a novel interfacial cross-linking method as a potential protein drug delivery system. *J. Pharm. Sci.* 2012; 101: 2177-2184.
55. Bonini M, Wiedenmann A, Baglioni P. Synthesis and characterization of magnetic nanoparticles coated with a uniform silica shell. *Mat. Sci. Eng.* C. 2006; 26: 745-750.
56. Chin AB, Yaacob II. Synthesis and characterization of magnetic iron oxide nanoparticles via w/o microemulsion and Massart's procedure. *J. Mat. Proc. Technol.* 2007; 191: 235-237.
57. Yilmaz H, Sanlier SH. Preparation of magnetic gelatin nanoparticles and investigating the possible use as chemotherapeutic agent. *Artif. Cells Nanomed. Biotechnol*. 2013; 41: 69-77.
58. Wang L, Wang Y, Wang X. synthesis and *in vitro* characterization of Fe^{3+}-doped layered double hydroxide nanorings as a potential imageable drug delivery system. Materials. 2017; 10 (10): 1-16.
59. Ren Y, Rivera JG, He L *et al*. Facile, high efficiency immobilization of lipase enzyme on magnetic iron oxide nanoparticles via a biomimetic coating. *BMC Biotechnol*. 2011; 11: 1-8.
60. Shukla A, Gundampati RK, Jagannadham MV. Immobilization of *Euphorbia tirucalli* peroxidase onto chitosan-cobalt oxide magnetic nanoparticles and optimization using response surface methodology. *Int. J. Biol. Macromol*. 2017; 102: 384-395.
61. Becheri A, Durr M, Nostro PL, Baglioni P. Synthesis and characterization of zinc oxide nanoparticles: application to textiles as UV-absorbers. *J. Nanopar. Res*. 2008; 10: 679-689.
62. Tang E, Tian B, Zheng E, Fu C, Cheng G. Preparation of zinc oxide nanoparticle via uniform precipitation method and its surface modification by methacryloxypropyltrimethoxysilane. *Chem. Eng. Commun*. 2008; 195: 479-491.

63. Yang J, Gao C, Lu S *et al*. Physicochemical characterization of amphiphilic nanoparticles based on the novel starch–deoxycholic acid conjugates and self-aggregates. *Carbohyd. Polym*. 2014; 102: 838-845.
64. Teodoro AP, Mali S, Romero N, de Carvalho GM. Cassava starch films containing acetylated starch nanoparticles as reinforcement: physical and mechanical characterization. *Carbohyd. Polym*. 2015; 1: 9-16.
65. Fan H, Ji N, Zhao M, Xiong L, Sun Q. Characterization of starch films impregnated with starch nanoparticles prepared by 2,2,6,6-tetramethylpiperidine-1-oxyl (TEMPO)-mediated oxidation. *Food Chem*. 2016; 1: 865-872.
66. Wang F, Yang S, Yuan J, Gao Q, Huang C. Effective method of chitosan-coated alginate nanoparticles for target drug delivery applications. *J. Biomat. App*. 2016; 31: 3-12.
67. Jiang DS, Long SY, Huang J, Xiao HY, Zhou JY. Immobilization of *Pycnoporus sanguineus* laccase on magnetic chitosan microspheres. *Biochem. Eng. J.* 2005; 25: 15-23.
68. Bi HY, Qiao L, Busnel JM, Liu BH, Girault HH. Kinetics of proteolytic reactions in nanoporous materials. *J. Proteom. Res*. 2009; 8: 4685-4692.
69. Querol E, Perez-Pons JA, Mozo-Villarias A. Analysis of protein conformational characteristics related to thermostability. *Protein Eng.* 1996; 9 (1996): 265-271.
70. Forootanfar H, Faramarzi MA, Shahverdi AR, Yazdi MT. Purification and biochemical characterization of extracellular laccase from the ascomycete *Paraconiothyrium variabile*. *Biores. Technol*. 2011; 102: 1808-1814.
71. Celis H, Romero I. The phosphate-pyrophosphate exchange and hydrolytic reactions of the membrane-bound pyrophosphatase of *Rhodospirillum rubrum*: effects of pH and divalent cations. *J. Bioenerg. Biomemb*. 1987; 19: 255-272.
72. Jaiswal N, Pandey VP, Dwivedi UN. Immobilization of papaya laccase in chitosan led to improved multipronged stability and dye discoloration. *Int. J. Biol. Macromol*. 2016; 86: 288-295.

How to cite this article:

Jagjit Kaur *et al*.2018, Immobilization And Characterization of L-Asparaginase Extracted From Solanum Nigrum on Magnetic Nanoparticles. *Int J Recent Sci Res.* 9(5), pp. 27199-27206. DOI: http://dx.doi.org/10.24327/ijrsr.2018.0905.2209

****